System Response Analyses of Base-Isolated Structures to Earthquake Ground Motions

C. Y. WANG, Y. TANG
Argonne National Laboratory , Argonne, IL USA
A. H. MARCHERTAS
Northern Illinois University, Dekalb, IL USA

1 INTRODUCTION

Seismic isolation is one of the most significant earthquake engineering developments in recent years. This paper describes system response analyses of base-isolated structures to earthquake ground motions. Emphasis is placed on the adaptation of a nonlinear constitutive model for the elastomeric isolation bearing together with the treatment of foundation embedment for the soil-structure-interaction analysis. The constitutive model requires six input parameters derived from bearing experimental data under sinusoidal loading. The characteristic behavior of bearing, such as the variation of shear modulus and material damping with the change of maximum shear deformation, can be captured closely by the formulation. In the treatment of soil embedment a spring method is utilized to evaluate the foundation input motion as well as soil stiffness and damping. The above features have been incorporated into a three-dimensional system response program, SISEC, developed at Argonne National Laboratory (ANL) (Wang et al. 1991). Sample problems are presented to illustrate the relative response of isolated and unisolated structures.

2 ANALYTICAL DEVELOPMENTS

2.1 Nonlinear viscoelastic constitutive model

The relationship between the applied displacement at one end of the elastomer bearing and the corresponding resultant force at the other end is essential for seismic analysis. Such a relationship under shear loading of composite isolation bearing has been successfully utilized at ANL. The constitutive relation for viscoelastic material usually involve the deformation gradient denoted by F. By polar decomposition the deformation gradient in turn can be directly related to the right Cauchy-Green tensor C as follows:

---

*Work performed under the auspices of the U.S. Department of Energy.

$$C = F^T F \,, \tag{1}$$

where the superscript T designates the transpose of a matrix. This tensor measures pure deformation. Similarly, with J denoting the determinant of F, the volume-preserving right Cauchy-Green tensor is given as

$$\bar{C} = CJ^{-2/3} \,. \tag{2}$$

In the viscoelastic constitutive formulation (Simo and Taylor 1985) the volumetric response of the material is assumed to be purely elastic; the viscoelastic effects are embodied by the deviatoric component. Their formulation is related to the second Piola-Kirchhoff stress tensor σ. The basic Simo-Taylor (S-T) constitutive model is expressed as a convolution integral of the form

$$\sigma(t) = K \ln J + \int_0^t \mu(t-s)\, \dot{\pi}\left[e(s),\varphi_t\right] ds \,, \tag{3}$$

where the first term on the right-hand side of Eq. (3) represents the volumetric component of stress and the second term stands for the deviatoric component. The bulk modulus K and the determinant of F (or det F) finalize the volumetric expression of the stress formulation.

Through a judicious selection of the nonlinear functions conforming to the physical material response of highly filled polymers, the solution of Eq. (3) replicates many of the characteristics of seismic bearings in shear under sinusoidal excitation. This was substantiated by a parameter study of the constitutive relation described above (Kim et al. 1991).

Note that the original S-T constitutive relation for shear loading requires five input parameters be specified. However, we have found from many numerical experimentations that a modified S-T constitutive model involving six parameters yields better results. In the modified model shown in Fig. 1, the first five parameters are derived from experimental plots of storage and loss moduli, the initial shear stiffness plus stiffness at very large strain, as well as the relaxation tests. The sixth parameter pertains to the weight ratio of the original relation to the nonlinear variable resistance in parallel.

2.2 Soil-structure interaction

A three-step spring method (Kausel et al. 1978) is adapted for the soil-structure interaction (SSI) analysis to treat a structure with deep foundation embedment and highly nonlinear isolation system. The first step calculates the foundation input motions (translation and rotation). The second step evaluates the impedance functions for the embedded foundation. The third step is using the

foundation input motion and impedance function as input to the SISEC code to perform the detailed SSI analysis.

Due to the presence of embedment, the foundation experiences not only horizontal translation motion, but also the rocking motion for a purely horizontal free-field motion. These horizontal and rocking motions, denoted by $X_i(t)$ and $\varphi_i(t)$, respectively, are given by:

$$\ddot{X}_i(t) = \mathrm{IFT}\begin{cases} \ddot{X}_g(\omega)\left[\cos\left(\frac{\pi}{2}\,\frac{f}{f_n}\right)\right] & \text{if } f \le 0.7\ f_n \\ \ddot{X}_g(\omega)[0.453] & \text{if } f > 0.7\ f_n \end{cases} \tag{4}$$

and

$$\ddot{\phi}_i(t) = \mathrm{IFT}\begin{cases} \ddot{X}_g(\omega)\left[0.257\left(1 - \cos\frac{\pi}{2}\,\frac{f}{f_n}\right)/R\right] & \text{if } f \le 0.7\ f_n \\ \ddot{X}_g(\omega)[0.257/R] & \text{if } f > 0.7\ f_n \end{cases}$$

where IFT stands for Inverse Fourier Transformation; $X_g(\omega)$ is the Fourier transform of the horizontal acceleration at the free surface in the free field, and f_n is the fundamental shear frequency of the embedment region.

To evaluate the impedance functions we assume the structural foundation is embedded in a homogeneous stratum. Let F and M be the horizontal force and rocking moment at the interface of the foundation and soil, X and ϕ be the corresponding lateral and rocking displacements, the force-displacement relationship can be written as

$$\begin{Bmatrix} F \\ M \end{Bmatrix} = \begin{bmatrix} K_{xx} & K_{x\phi} \\ K_{x\phi} & K_{\phi\phi} \end{bmatrix} \begin{Bmatrix} X \\ \phi \end{Bmatrix}, \tag{5}$$

where K_{xx} $K_{x\phi}$, and $K_{\phi\phi}$ are the impedance functions. These coefficients generally are functions of the soil shear modulus, radius of the foundation, depth of the embedment, and the depth of bedrock, soil Poisson's Ratio, etc. (Kausel et al. 1978).

3 RESULTS AND DISCUSSIONS

3.1 Validation of viscoelastic constitutive equation

A 1/4-scale test of an elastomeric bearing was performed at the Earthquake Engineering Research Center (EERC), University of California-Berkeley for the PRISM Liquid Metal Reactor Project (Tajirian and Kelly 1988). In the test a sinusoidal shear loading is applied at the top of the isolator. A typical experimental hysteresis loop of the 1/4-scale bearing is shown in Fig. 2. Numerical simulation of the scale model test was accomplished by running a one-element problem within the SISEC code. The hysteresis loops of analytical model due to pure sinusoidal input is given in Fig. 3. As can be seen, the agreement of force-displacement relationships between the experimental and analytical results is quite good.

3.2 Responses of unisolated and isolated structures under horizontal excitation

The finite-element model of a nuclear island is shown in Fig. 4. Two lumped-mass sticks are used to model the reactor containment and reactor building. Two calculations are performed dealing with unisolated and isolated plants, respectively. For the unisolated plant, one foundation mat is utilized. On the other hand, the isolated plant has two concrete foundation mats, and the isolators are placed between these two mats. The design fundamental frequency of the isolators is 0.50 Hz.

In calculating the response of the isolated structure, the isolators are modeled by two spring elements, one linear spring for simulating the large vertical stiffness and one nonlinear viscoelastic spring for modeling the relatively low stiffness in the horizontal direction. For simplicity, only one composite isolator representing the global effect of the estimated 600 isolators is used in the analysis. The free-field artificial input acceleration history has a peak ground acceleration of 0.20 g.

Maximum accelerations at node 1 (basemat), 23 (top of containment) and 43 (top of the reactor building) are useful for studying the relative merit of the high damping base-isolation system. For the unisolated plant, the peak accelerations of these three locations are 0.22 g, 0.43 g and 0.33 g.

However, for the isolated structure, the maximum accelerations at nodes 1, 23, and 45 are about 0.083 g, 0.0875 g, and 0.085 g, respectively. Note that because of softness of the isolator bearings in responding to the horizontal excitation, the peak accelerations at these three locations are much smaller than that of the input ground acceleration, 0.20 g. In other words, by using the high damping elastomeric bearings the superstructure is basically decoupled from the ground motion during the earthquake. For illustration of the mitigating effect of elastomer bearings, comparison of acceleration histories at node 23 (top of the reactor containment) of the unisolated and isolated plants is given in Fig. 5. Figure 6 displays the hysteresis plots of the composite bearing. The energy absorbed by the bearing is shown in Fig. 7.

REFERENCES

Wang, C. Y. et al. (1991). Seismic Analyses of Base Isolated Structures with High Damping Elastomeric Bearings, in Seismic Engineering, Proc. ASME PVP Conference.

Simo, T. C. and Taylor, F. L. (1985). A Three-Dimensional Finite Deformation Viscoelastic Model Accounting for Damage Effects, Report No. UCB/SESM/85-02, SESM, University of California-Berkeley.

Kim, M. J., Gupta, A. and Marchertas, A. H. (1991). Utilization of the S-T Viscoelastic Constitutive Model for the Simulation of Isolation Bearing, Trans. SMiRT-11, paper K 23/4.

Kausel, E. et al. (1978). The Spring Method for Embedded Foundations, Nucl. Eng. & Design, Vol. 48, pp. 377-392.

Tajirian, F. F. and Kelly, T. M. (1988). Testing of Seismic Isolation Bearings for Advanced Liquid Metal Reactor PRISM, in Seismic, Shock, and Vibration Isolation - 1988, ASME Publication, PVP - Vol. 147.

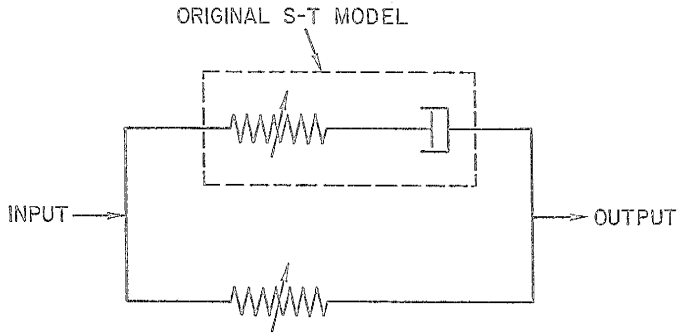

Fig. 1 Modified S-T Constitutive Model

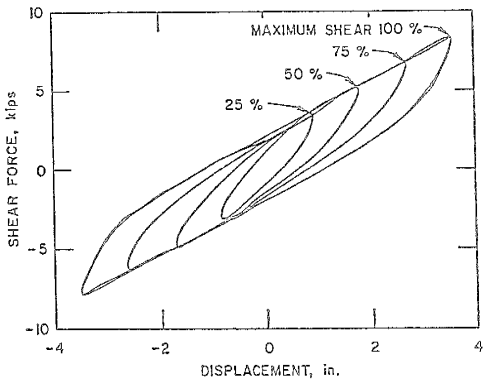

Fig. 2 Typical Hysteresis Loop of 1/4-Scale PRISM Bearing

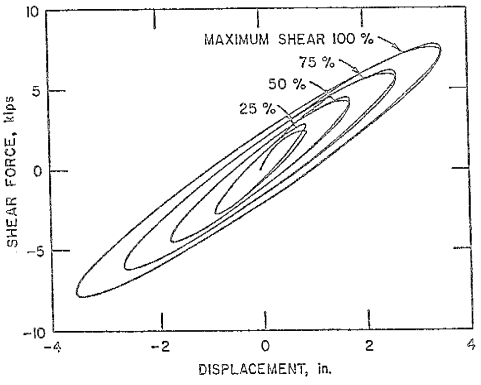

Fig. 3 Hysteresis Loop of Analytical Model

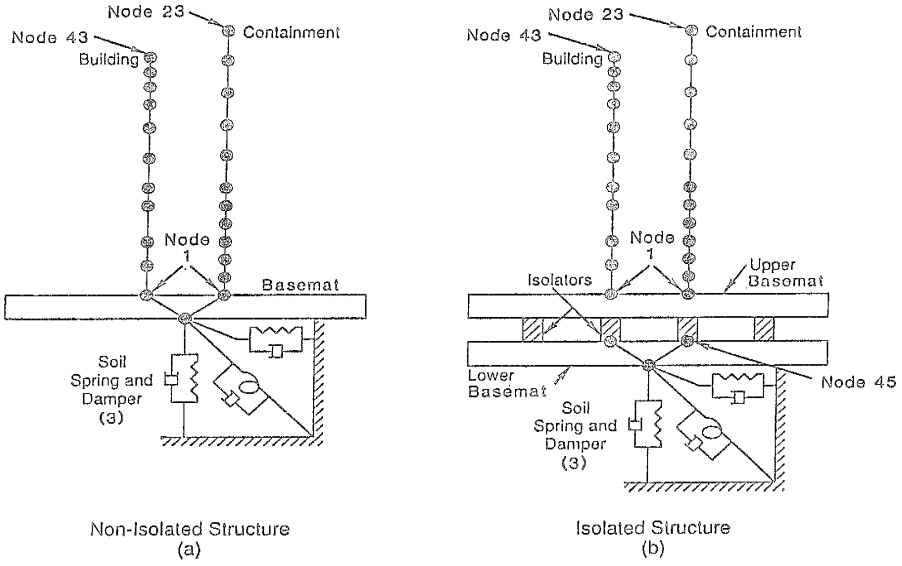

Fig. 4 Finite-Element Model of a Nuclear Island

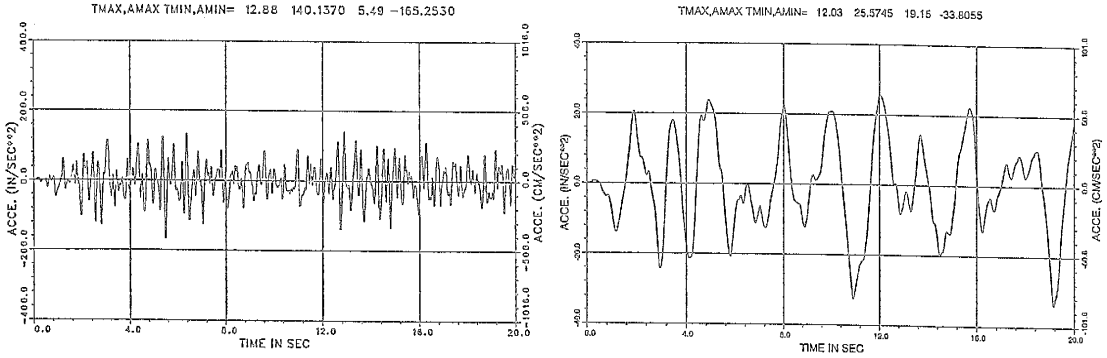

Fig. 5 Acceleration Histories at the Top of Containment (left: unisolated, right: isolated)

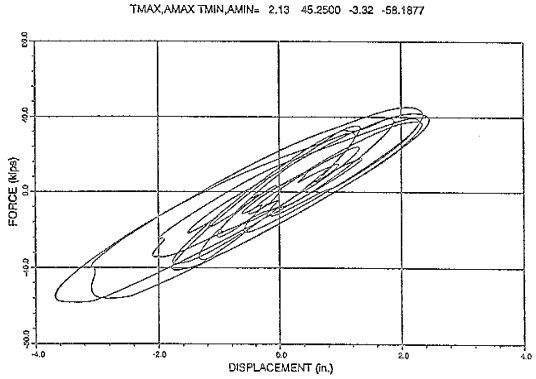

Fig. 6 Hysteresis Loop of a Composite Bearing

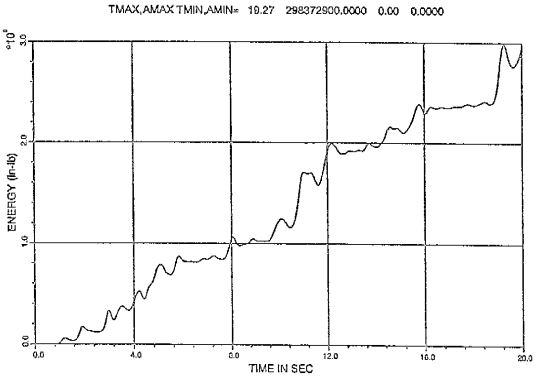

Fig. 7 Energy Absorbed by the Bearing